acta phys. slov. 26 (1976), No. 4

THE RHO POLE PARAMETERS

JURAJ BOHÁČIK,* Bratislava

The application of the analytic extrapolation method for testing the hypothesis of two complex conjugate poles on the second sheet of a $\pi\pi$ P-partial wave amplitude is studied. Numerical values of the pole parameters depend to some extent on the set of phase shifts used in the analysis. The hypothesis of two conjugate poles on the second sheet in the $\pi\pi$ P-wave has high confidence levels for all data sets used.

The resulting values of the pole parameters are in the energy regions M: 753—770 MeV, $\Gamma/2$: 71—83 MeV.

ПАРАМЕТРЫ ПОЛЮСА ϱ-РЕЗОНАНСА

Изучается возможность использования метода аналитического продолжения для проверки гипотеза о существовании двух комплексно-сопряжённых полюсов на втором листе парциальной амплитуды $\pi\pi P$ рассеяния. Числовые значения параметров полюса зависят в некоторой степени от набора сдвигов фаз, которые используются в анализе. Гипотеза о двух сопряжённых полюсах на втором листе в $\pi\pi P$-волне имеет большую степень достоверности для всего набора используемых данных.

Полученные значения параметров полюса находятся в области энергий: $M \sim 753$—770 Мэв, $\Gamma/2 \sim 71$—83 Мэв.

I. INTRODUCTION

Recently several papers have appeared dealing with resonance pole positions on the second sheet of $\pi\pi$ partial wave amplitudes (p.w.a). For experimental data they use the modern $\pi\pi$ p.w.a. analyses [4, 12]. Usually the Breit—Wigner formulas modified by some model assumptions plus smooth background terms are used for fitting the data in certain energy intervals around the resonance. In this paper we shall present the results obtained by a method based on the analytical properties of the amplitude. This method gives by using the Cauchy integral directly the pole position. In order to test how the method works in the $\pi\pi$ case, we confine ourselves to the rhomeson pole position.

* Institute of Physics of the Slovak Academy of Sciences, Dúbravská cesta, 899 30 BRATISLAVA, Czechoslovakia.

The method is described in [1, 2]. It was used by Nogová, Pišút [3] for the determination of the pole parameters of the $\Delta(1236)\pi N$ resonance. The method is in principle model independent and its application on the p.w.a. data will give the answers to the two following questions [2]: (i) do the data for certain p.w.a. imply the presence of a resonance pole (poles) on the second sheet? (ii) if yes, what is the position of this pole (poles) in the complex s-plane? We shall assume that the rho-resonance can be described by two complex conjugate poles on the second sheet.

The paper is organized as follows. The next section contains a short description of the method, the construction of the amplitude on the second sheet and the conformal mapping onto the unit disc. In Sect. III. the method is applied to the simple model example of the p.w.a. Sect. IV. contains the results obtained from data on $\pi\pi$ P-wave analyses [4, 5]. Discussion of results is presented in Sect. V. In the Appendix we describe the construction of the weight function.

II. THE METHOD

Here we describe very briefly the main ideas of the statistical method of analytical continuations and how it works in our case.

Let us suppose that we have conformally mapped the second sheet of p.w.a. in the s-plane onto the unit disc in the z-plane. Let $F(z)$ be a function holomorphic on the unit disc, belonging to the Hilbert space $\mathscr{H}$ of quadratic integrable functions on the unit circle. Let $Y(z)$ and $\varepsilon(z)$ be smooth interpolations of data and weighted errors on the unit circle $|z|=1$. The unnormalized probality in $\mathscr{H}$ is

$$P(F) \sim \exp\{-\tfrac{1}{2}\chi_c^2\}, \qquad (1)$$

where

$$\chi_c^2 = \frac{1}{2\pi}\oint_c \frac{|F(z)-Y(z)|^2}{\varepsilon(z)^2}|dz|;$$

c is the unit circle $|z|=1$.

We can interpret the probability $P(F)$ as follows: We shall suppose that the analytical properties of $F(z)$ are known. Eq. (1) gives the probability distribution for different experimental outcomes, represented by $Y(z)$. We introduce the weight function $g(z)$, which is meromorphic and free of zeros in $|z|<1$. On the unit circle $|z|=1$ we have

$$|g(z)| \approx \varepsilon(z)$$
$$\varepsilon(z_i) \approx |\Delta_i|(2\pi\varrho_i)^{-1/2} \qquad (2)$$

here Δ_i are the experimental errors; ϱ_i the density of data points around z_i; z_i the mapped i-th data points from the s-plane. We can define

$$f(z) = F(z)/g(z)$$
$$y(z) = Y(z)/g(z) \qquad (3)$$

the meromorphic functions in the unit disc. Now we expand (3) into the Laurent series. When we assume that $F(z)$ has two complex conjugate poles, we can write:

$$f(z) = \frac{\alpha}{z-\lambda} + \frac{\alpha^*}{z-\lambda^*} + \sum_{n=0}^{\infty} a_n z^n = \sum_{n=1}^{\infty} 2\mathrm{Re}(\alpha\lambda^{n-1})z^{-n} + \sum_{n=0} a_n z^n \qquad (4)$$

$$y(z) = \sum_{-\infty}^{\infty} y_n z^n. \qquad (5)$$

Inserting (4, 5) into (1) we get:

$$\chi_c^2 = \sum_{n=1}^{\infty}[2\,\mathrm{Re}(\alpha\lambda^{n-1}) - y_{-n}]^2 + \sum_{n=0}^{\infty}(a_n - y_n)^2; \qquad (6)$$

here we define

$$Q_n \equiv y_{-n} = \frac{1}{2\pi}\oint_c \frac{Y(z)}{g(z)} z^n |dz|. \qquad (7)$$

Using the real analyticity of p.w.a. we shall suppose that Q_n, a_n, y_n are real. Assuming that $F(z)$ is really determined by data according to (6) we see that the quantity

$$\sum_{m+1}^{N+m} |Q_n - 2\,\mathrm{Re}(\alpha\lambda^{n-1})|^2$$

has a chi-squared distribution with N-5 degrees of freedom [11].

The method cannot tell us unambiguously what kind of singularities the p.w.a. possesses. It gives answers of the same kind as any statistical hypotheses testing would give. We thus can learn whether a given type of singularity is consistent with the data but not whether this is a unique solution. The method which we shall use here is free of ambiguities connected with the resonance-background separation.

We shall test the hypothesis about two complex conjugate poles on the second sheet in the $\pi\pi$ P-p.w.a. Using the data and assumptions about low- and high-energy behaviour of the p.w.a., we shall construct the p.w.a. on the first sheet in the physical region ($s \geq 4\mu^2$) in the following way.

1) We use the simplest expansion for the phase shift in the region between the physical threshold and the first data point:

$$\delta(s) = a_1^1 q^{2l+1} + Bq^{2l+3} + Cq^{2l+5} \qquad (8)$$

here $l=1$; a_1^1 is the scattering length; q the π momentum in cms.

The scattering length parameters were taken from the low energy calculations by the Roy equation [6, 8]. We find the coefficients B, C from the requirement

$$\delta(s_i) = \delta_i \qquad i = 1, 2;$$

δ_i is the experimental phase shift in the i-th data point; s_i — cms total energy square for the i-th data point.

2) We use the linear interpolation of the nieghbourhood δ_i, η_i in the region where we have the data.

3) In the high energy region, where due to unitarity the following formula is valid

$$|f_l^l(s)| \leq \frac{1}{\sqrt{s}}$$

we shall use:

$$f_l^l(s) = f_l^l(s_{max}) \frac{q(s_{max})}{q(s)}, \qquad s > s_{max};$$

s_{max} is the highest data point.

Now on the first sheet for $s \leq s_{max}$ the p.w.a. is given by

$$f_l^l(s) = \frac{\eta(s)\, e^{2i}\delta(s) - 1}{2iq(s)}. \tag{9}$$

The second sheet amplitude Y is obtained by crossing the elastic part of the physical cut

$$Y(s) \equiv f_l^{l\,(II)}(s) = \frac{f_l^l(s)}{1 + 2iq(s) f_l^l(s)} \tag{10}$$

$Y(s)$ has two cuts $(-\infty; 0)$ and $(4\mu^2; \infty)$ on the second sheet. The mapping of the second sheet onto the unit disc is done in two steps.

i) First we transform the s-plane into the v-plane:

$$v = \frac{s - 2\mu^2}{2} \tag{11}$$

ii) Secondly, we map the v-plane with two cuts $(-\infty; -\mu^2)$ and $(\mu^2; \infty)$ onto the unit disc in the z-plane:

$$z = \frac{1 - \sqrt{1-v}\sqrt{1+v}}{v}. \tag{12}$$

The situation in the z-plane is shown in Fig. 1.

Now we can compute the Q_n coefficients using relation (7). We shall neglect the contribution from the left part of the circle $|z| = 1$ in this paper. Therefore we require that $g(z)$ has the large values on this part of the unit circle. Unlike paper [3], where $g(z)$ was the oscillating function on the whole circle $|z| = 1$, we use a $g(z)$ which is oscillating only on the part of the unit circle and it is real elsewhere on

this circle. The construction of $g(z)$ is described in the appendix. The number N is the characteristic value of $g(z)$. The values of $g(z)$ are higher on the left half circle when N increases.

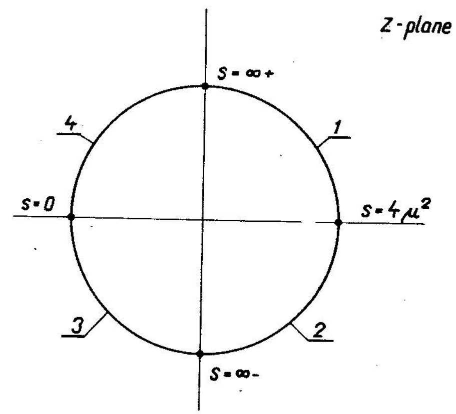

Fig. 1. Transformation of the s-plane onto the unit disc in the z-plane; 1 — image of the upper bank of the right-hand cut in the s-plane; 2 — image of the lower bank of this cut; 3 — image of the lower bank of the left-hand cut; 4 — image of the upper bank of this cut.

Because the integrand in (7) is a real analytic function, we can rewrite (7) as:

$$Q_n = \frac{1}{\pi} \int_0^{\pi/2} \mathrm{Re} \left\{ \frac{Y(z)}{g(z)} z^n \right\} |dz|. \tag{13}$$

In (13) the amplitude on the left half circle was approximated by zero.

The pole position is determined by minimizing the quantity

$$\chi^2 = \sum_{n=m+1}^{N+m} |Q_n - 2\,\mathrm{Re}(\alpha\lambda^{n-1})|^2. \tag{14}$$

At the preliminary stage it is possible to estimate the pole position by using the equations:

$$Q_{n+i} = 2\,\mathrm{Re}(\alpha\lambda^{n+i-1}) \qquad i = 0, 1, 2, 3. \tag{15}$$

Putting $\lambda = \lambda_1 + i\lambda_2$ we have

$$\lambda_1 = \tfrac{1}{2}(Q_{n+1}Q_{n+2} - Q_nQ_{n+3})(Q_{n+1}^2 - Q_nQ_{n+2})^{-1}$$
$$|\lambda|^2 = (Q_{n+2}^2 - Q_{n+1}Q_{n+3})(Q_{n+1}^2 - Q_nQ_{n+2})^{-1}. \tag{16}$$

We shall use the pole positions computed by (16) for various n for the estimate of the errors of λ_1 and λ_2 (i.e. the mass and the halfwidth of the resonance — pole position) computed by (14), and for the discussion of the method used.

III. TESTING THE METHOD BY USING THE EXAMPLE OF A P.W.A. WITH A RESONANCE ON THE SECOND SHEET

A model containing a pair of the complex conjugated resonance poles on the second sheet is constructed by writing the p.w.a. in terms of suitably parametrized Jost functions [3]. For the $\pi\pi$ case we define:

$$S(k)=f(k)/f(-k)$$
$$f(k)=(k-a-ib)(k+a-ib)\,. \tag{17}$$

For the p.w.a. on the first sheet we shall put

$$F(s)=\frac{S(k)-1}{2iq} \tag{18}$$

$$k(s)=\tfrac{1}{2}\sqrt{s-4\mu^2}$$
$$q(s)=k(s)\,.$$

The function $k(s)$ possesses in the s-plane the analytic property:

$$k(s)=-k^*(s^*)\,.$$

$F(s)$ is a real analytic function in the s-plane. The corresponding branch on the second sheet $F^{\mathrm{II}}(s)$ has two complex conjugated poles at s_R and s_R^*:

$$s_R\equiv s_1+is_2=4\mu^2+4(a^2-b^2)+i8ab\,. \tag{19}$$

The parameters of the Jost functions a and b are fixed by the following requirement:

$$s_R=(M_r+i\,\Gamma/2)^2$$
$$M_r=750\ \mathrm{MeV} \tag{20}$$
$$\Gamma/2=\ 55\ \mathrm{MeV}\,.$$

The phase shift of $F(s)$ is

$$\delta(s)=\operatorname{arctg}\left(\frac{2bk(s)}{a^2+b^2-k^2(s)}\right)\,. \tag{21}$$

The scattering length-like parameter from (21) is:

$$a_1^1=\frac{2b}{a^2+b^2}\,.$$

Using (21) we produce δ_i for those s_i, where the experimental data are known from phase shift analyses [4, 5]. From these δ_i and a_1^1 given by (22) we can construct the function $Y(z)$ (see Eq. (10)) by the prescriptions of part II. Constructing the weight functions for these trial examples we take into account the

experimental errors of the phase shift analyses used. The pole positions of the Jost function will be determined by using (16). The results are in the Figs. 2, 3, 4. The pole positions found by the method described agree well with the true pole position of $F(s)$. The real part of the pole position ($\equiv$mass) is determined better than the imaginary part ($\equiv$halfwidth). It is probably due to the neglecting of contributions

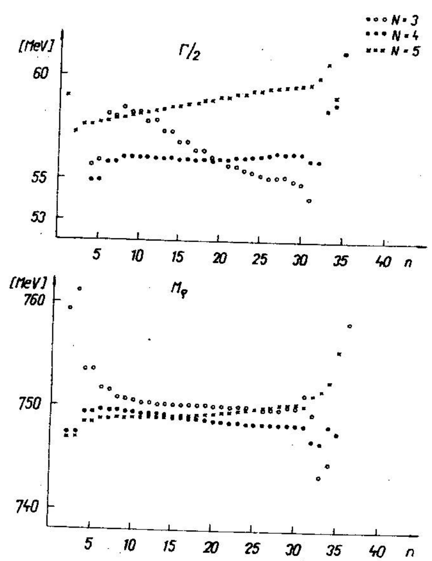

Fig. 2. The results of the trial example. Protopopescu et al. [4]; the energies data points are used.

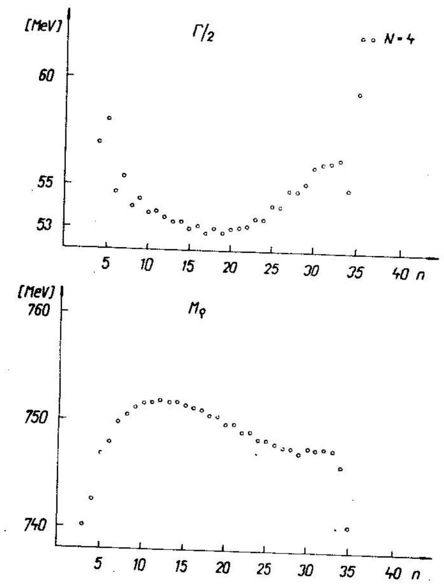

Fig. 3. The results of the trial example. Estabrooks et al. [5]; the energies data points are used for the elastic case only.

from the left part of the unit circle $|z|=1$, as a very small part of the data region on the unit circle. In Tab. 1 there are arguments of complex points $z(s_1)$ and $z(s_{max})$ for the data analyses used. When the N for the weight function is increased, the neglecting of the left-part of the unit circle contribution is more reasonable. The significance of the data area is increased in this way, but the errors from this region play a more important role too. It seems therefore that it is necessary to make a compromise between suppressing $Y(z)$ on the left part of the circle $|z|=1$ and the numerical integration of the oscillating function as well as the increasing role of the uncertainties in the p.w.a. data.

Table 1

Arguments of the first and the last energy point transformed on the $|z|=1$ circle for the data sets used

Data analysis	$\varphi(s_1)$ [deg]	$\varphi(s_{max})$ [deg]
Protopopescu et al. [4]	81.438	88.250
Estabrooks et al. [5] elast. data only	76.111	87.508
all data without lowes energies	82.709	88.766

IV. RESULTS

The weight functions, which work well for the trial examples were used for the P-p.w.a. of the $\pi\pi$ data [4, 5]. We emphasize the statistical feature of our results concerning the type of singularity on the second sheet.

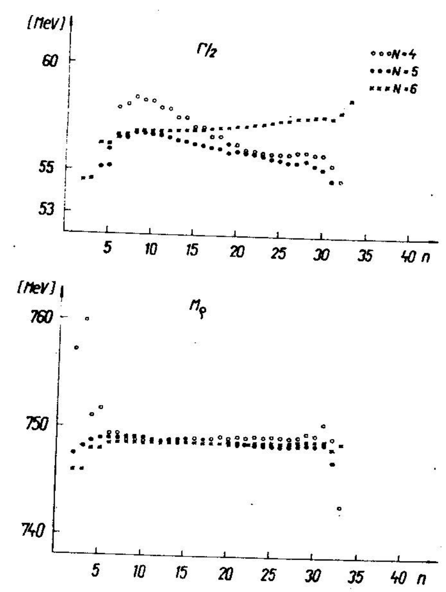

Fig. 4. The results of the trial example. Estabrooks et al. [5]; the energies data points are used, both elastic and nonelastic, excluding the data points for energies lower than 590 MeV.

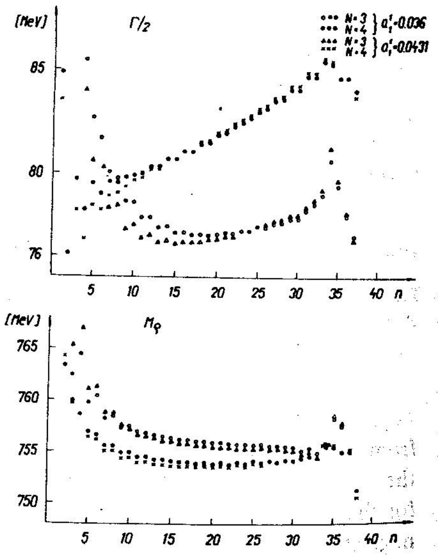

Fig. 5. Pole position using the SDPI data and relation (16). When the distance between the points with the distinct scattering length is lower than 0.1 MeV, we draw only the point with $a_1^1=0.036$.

We used two data sets from the analysis by Protopopescu et al. [4]. The first data set (here denoted as SDPI) is in Tab. VI [4], denoted there as "case 1". The second data set (SDPII) was obtained from the first one by replacing the higher energy data by the data of Tab. XIII [4]. The two data sets are both model and extrapolation mode dependent. The results obtained by Eq. (16) are in the Figs. 5, 6. We suppose that the increase of $\Gamma/2$ with an increasing n could indicate

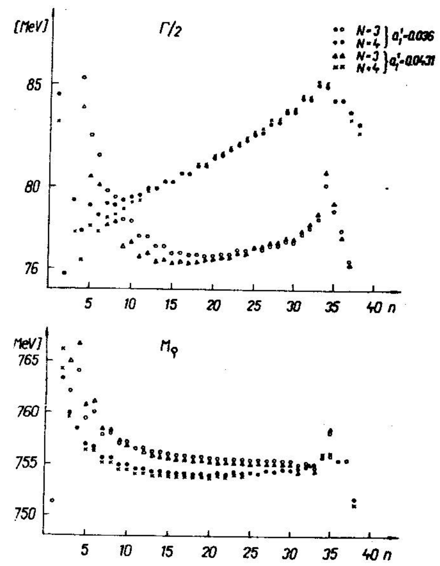

Fig. 6. Pole position using the SDPII data.

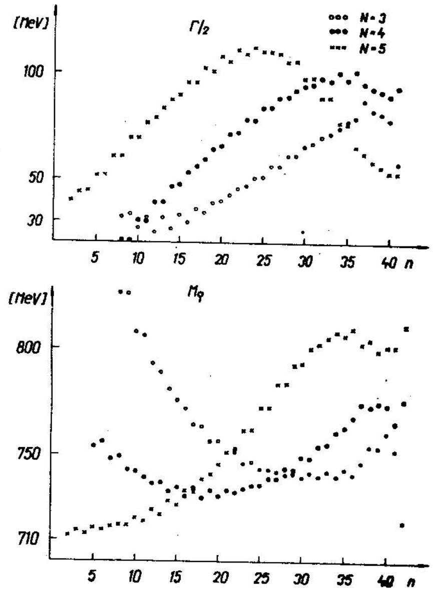

Fig. 7. The results using the Estabrooks et al. [5] elastic data.

some systematic error of the data. Using (14) we obtain results which are summarized in Tab. 2. The errors in M and $\Gamma/2$ are chosen with regard to Figs. 5, 6. The confidence level is interpreted as the probability of rejecting the reasonable hypothesis [11]. Two different values of scattering are used. Pennington and Protopopescu [6] refer to the value $a_1^1=0.036$. This values was obtained by usung the Roy equations and data [4] used here. As the other value $a_1^1=0.0431$ we take the higher and very different value from Basdevant et al. [8]. In Figs. 5, 6 we see that our results are not very sensitive to the different values of the scattering length in the interval $9 \leq n \leq 35$.

In Fig. 7, there are the results obtained by using the elastic data of the P-p.w.a. analysis of Estabrooks et al. [5]. Here is used the scattering length [9] $a_1^1=0.038$.

Table 2

Pole parameters and associated confidence levels for three data sets used. The errors ±10 MeV are estimated using the results of the Figs. 5, 6, 8. These errors are not statistical but take into account the results with the different values of the parameter N

Data	M[MeV]	$\Gamma/2$ [MeV]	χ^2	confidence level	number of used Q coefficients
SDP I	755.6±10	83 ±10	0.01	0.95	27
SDP II	753.7±10	82±10	0.003	0.97	27
Estabrooks et al.	769.7±10	71.6±10	0.03	0.9	27

The values of $M\varrho$, $\Gamma/2$ have a considerable dispersion in this case. Petersen [9] showed that data [5] are inconsistent for low energies (<600 MeV). We suppose that this dispersion is due to that inconsistency. In Fig. 8 there are results obtained by data [5] for both elastic and nonelastic cases. The data for energies lower than 590 MeV are not taken into account. In Tab. 2 there are results obtained by Eq. (14) for this case. Data [5] are model dependent, too.

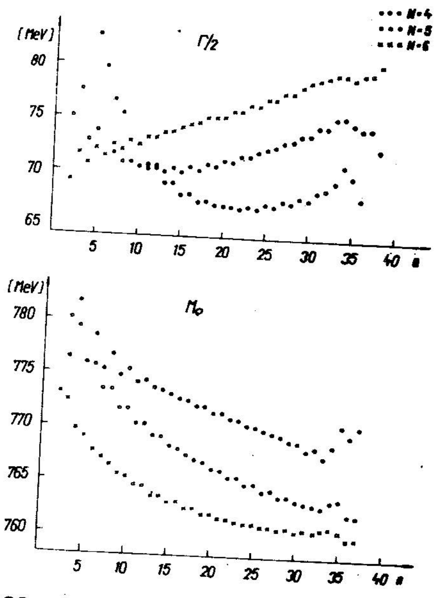

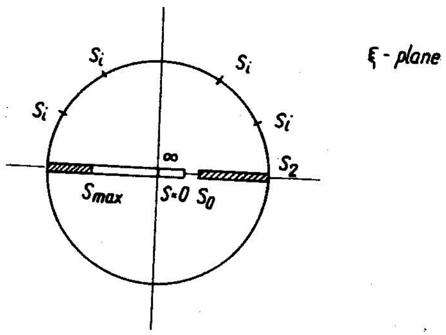

Fig. 9. Transformation of the s-plane onto the unit disc in the ξ-plane; s_i — images of the experimental data points or the (s_0, $s=0$, ∞) significant points from the s-plane.

Fig. 8. Results using the Estabrooks et al. [5] both the elastic and the non-elastic data excluding lower than 590 MeV energy data points.

V. DISCUSSION

The method used here for the determination of rho-meson pole parameters does not give the unambiguous answer about the type of singularity on the second sheet of the p.w.a. It enables us to examine the consistency between the data and the supposed type of singularity. The important parameter is the confidence level (see Tab. 2). We see that the hypotheses of two complex conjugate poles on the second sheet of the P-p.w.a. have a high confidence level for all the data sets used. The pole positions are different for the different data sets. It seems to the author that it is due to the model dependence of the $\pi\pi$ phase shift analyses used.

When we compute the Q_n with a high n, we meet the problem of integration of highly oscillating functions. It is therefore reasonable to use only a limited number of Q_n coefficients.

The parameters of the rho meson pole are in good agreement with the results of the other authors (see Tab. 3). We believe that better results would be obtained by taking into account the contribution from the left part of the unit circle.

Table 3

Comparison of our results and results of other authors. The numbers in squared brackets are reference numbers. Our results are in the columns denoted as SDPI, SDPII, and „Estabrooks et al.“

	SDP I	SDP II	Estabrooks et al.	[4]	[5]	[10]	[12]
M[MeV]	755.6±10	753±10	769.7±10	755±4	722 ±0.6	757±2	778±2
$\Gamma/2$ [MeV]	83 ±10	82±10	71.6±10	80±5	71.55±0.55	81±2	76±1

The numerical calculations were made in the Institute of Computer Sciences of the Comenius University, Mlynská dolina.

ACKNOWLEDGEMENT

I wish to thank J. Pišút for turning my attention to this problem and for numerous useful discussions. I am indebted to H. Kühnelt for valuable discussions and correspondence and A. Nogová for useful conversations and for reading the manuscript.

APPENDIX

We construct the weight functions by the method due to F. Elvekjaer [7]. We transform the complex s-plane onto the unit disc in the ξ-plane as follows:

$$t = -s + \text{const.} \tag{A.1}$$

$$v = t_0/(t_0 - t) \tag{A.2}$$

$$\xi = \frac{1 - \sqrt{1-v}\sqrt{1+v}}{v}. \tag{A.3}$$

This transformation transforms the point $s = \text{const.}$ into the point $\xi = 1$, the point $s = (\text{const.} - 2t_0)$ into the point $\xi = -1$. The point $s = \infty$ is transformed into the point $\xi = 0$ (see Fig. 9).

In the ξ-plane we define the polynomial

$$W^N_{(\xi)} = \sum_{n=0}^{N} a_n \xi^m. \tag{A.4}$$

We require that $W^N_{(\xi)}$ fulfil the condition:

$$[W^N_{(\xi)}]^{-1} \neq 0, \qquad |\xi| \leq 1.$$

The function $W^N_{(\xi)}$ possesses in the s-plane the cut in the interval $s \in (\text{const}; \text{const} - 2t_0)$. In the other part of the s-plane the real axis $W^N_{(\xi)}$ is a real and decreasing function.

Let us put

$$g(s) = [W^N_{(\xi)}]^{-1}. \tag{A.5}$$

We determine the values of the parameters "const.", "t_0" and "a_n" in the relations (A.1—A.4) as follows.

i) We require to suppress the high, low energy data region as the left hand cut region in the s-plane. We put the const. $= s_2$ (i.e. the square of the total energy in the second data point), $2t_0 = t(s = 4\mu^2) + t(s_{max})$ (i.e. the images of the s-channel physical threshold and the last data point are on the real axis in the unit disc $|\xi| \leq 1$ and there are applied

$$|\xi(4\mu^2| = |\xi(s_{max})| < 1).$$

ii) The theory of meromorphic functions enables us to construct the polynomial (i.e. the analytical function in the complex plane), which approximates a continuous function on some curve P. We can approximate this function to an arbitrary accuracy when this curve does not divide the complex plane into two disjoint components.

We require that

$$|g(s_i)| \approx |\Delta_i| / \sqrt{2\pi\, \varrho_i} \tag{A.6}$$

here

$$\Delta_i = \left|\frac{\partial f^{II}(s_i)}{\partial \delta}\right| \Delta\delta_i + \left|\frac{\partial f^{II}(s_i)}{\partial \eta}\right| \Delta\eta_i \tag{A.7}$$

f^{II} — p.w.a. on the second sheet; $\Delta\delta_i$, $\Delta\eta_i$ — experimental errors of the phase shift and elasticity, respectively; ϱ_i — the density of the data points on the unit circle in the z-plane around z_i (see [2, 3]).

The data points are in the ξ-plane on the upper part of unit circle $|\xi| = 1$. The ξ-plane is not divided by this curve. We can fulfil (A.6) using (A.5) and (A.4) with an arbitrary accuracy. Due to the model dependence of the phase shift analyses used, we use in (A.5) only one term of the polynomial (A.4). We have

$$|a_N \xi^{-N}_{(s_i)}| \approx |\Delta_i| / \sqrt{2\pi\, \varrho_i}. \tag{A.8}$$

We use the relation (A.8) for determining the weight function.

REFERENCES

[1] Nogová A., Pišút J., Prešnajder P., Nucl. Phys. B *60* (1973), 548.
[2] Pišút J., *On the Statistical Description of Scattering Amplitudes by Analytic Functions.* Lecture at the Xth Winter School of Theoretical Physics, Karpacz, 1973.
[3] Nogová A., Pišút J., Nucl. Phys. B *61* (1973), 445.
[4] Protopopescu S. D. et al., Phys. Rev. D *7* (1973), 1279.
[5] Estabrooks P. et al., *ππ Phase Shift Analysis.* Ref. TH. 1661 — CERN.
[6] Penington I., Protopopescu S. D., Phys. Rev. D *7* (1973), 1429.
[7] Elvekjaer F., Nucl. Phys. B *43* (1972), 445.
[8] Basdevant I. L., Froggatt C. D., Petersen J. L., Nucl. Phys. B *72* (1974), 413.
[9] Petersen J. L., *Status of Meson-Meson Interaction.* Nordita. Copenhagen, January 1974.
[10] Arnd R. A., Hackman R. H., Roper L. D., *Pole Position for the f and g mesons.* VPIMT — 3 (74).
[11] Hudson D. J., *Statistics. Lectures on Elementary Statistics and Probability.* Geneva 1964.
[12] Hyams B. et al., Nucl. Phys. B *64* (1973), 132.

Received June 26th, 1975